Special issue in honour of Prof. Reto J. Strasser

Phosphorus deficiency affects the I-step of chlorophyll *a* fluorescence induction curve of radish

M.D. CETNER[*,+], H.M. KALAJI[*], W. BORUCKI[**], and K. KOWALCZYK[***]

Department of Plant Physiology, Institute of Biology, Warsaw University of Life Sciences WULS-SGGW, 159 Nowoursynowska Street, 02-776 Warsaw, Poland[*]
Department of Botany, Institute of Biology, Warsaw University of Life Sciences WULS-SGGW, 159 Nowoursynowska Street, 02-776 Warsaw, Poland[**]
Department of Vegetable and Medicinal Plants, Institute of Horticulture Sciences, Warsaw University of Life Sciences WULS-SGGW, 166 Nowoursynowska Street, 02-787 Warsaw, Poland[***]

Abstract

radish plants.

Additional key words

Introduction

Phosphorus (P) is one of the essential nutrients that

is worldwide common, covers an area of over 2 billion ha

(Fairhurst *et al*

et al. 2018). On other hand, in some parts of the world P fertilisers are overused causing severe eutrophication (MacDonald *et al*. 2011). Thus, considering

Received 15 November 2019, *accepted*

[+] magdalena.cetner@gmail.com

Abbreviations b_6f b_6f 0 A^- m + $_O = F_{0.05ms}$ – minimal 0 $_A$ reduction events between time 0 and T_{Fm} Mn_4CaO_5 abs B tot $_A$ reducing RCs per PSII antenna 0 0 T_{Fm} 0 R0 B E0 P0 R0 E0 A^-.

Acknowledgements
M00261-99).

fertilisers, is a nonrenewable resource, sustainable use

et al. 2015).

nucleic acids, nucleotides, phosphoproteins, phospholipids

(Malhotra *et al.* 2018). Both inorganic and organic

cellular pH. Inorganic phosphate (Pi) is able to form water-

diphosphate) and ATP (adenosine triphosphate), which are

processes.

see

e.g

see e.g.,

membrane, which is the accumulation of H^+

lumen and the decrease of H^+ in the chloroplast stroma,

26 0 04C00330055005200570052005100003>11.7 0 04A008004F004800460057005500520051000323.6 0 00003>11.7i97Tm[(26 0 04C00

to learn about the content of phosphorus in their tissues (Malhotra *et al.*

be used for assessing plant phosphorus status on-site. *et al.*

see Strasser *et al.*

was applied to get better understanding of the impairment

radish plants.

Materials and methods

Plant material and growth conditions: Two radish *Raphanus sativus* var. *sativus* 'Suntella

growth chamber under a set of controlled conditions, close to optimal for both cultivars. The photoperiod was 14 h

s

Kalaji team invention).

tap water. After that time, the control solution (optimal

i.e. th
17th d of vegetation was the 1st d after treatment (1 DAT).

rd d of vegetation, *i.e.*, 27 DAT.

loped based on the Hoagland solution (Hoagland and Arnon 1950). The control medium contained the following $^{-1}$):
N (as NO_3 4 4 3
NH_4 4 4 $^{-1}$

0.52. For details, *see* Tables 1S and 2S (*supplement*). All

Measuring methods and devices

period, *i.e.*, at 3, 6, 12, 19, and 25 DAT. There were 3 to

Vario Max CN Element Analyzer, Elementar Analysensysteme GmbH

Thermo Scientific iCAP 6000, *Thermo Fisher Scientific Inc.* 3
$HClO_4$ (HNO_3:$HClO_4$

each term, cultivar, and treatment.

(P_N), transpiration rate (E), stomatal conductance (g_s), and intercellular CO_2 concentration (C_i) were evaluated *in vivo* *LCpro+* (*ADC BioScientific Ltd.*, UK). Measurements were conducted four times during the vegetative period, on 5, 10, 17, and

Measurements were conducted under ambient light in the s] and CO_2 concentration *ca*. 400 ppm. Samples were closed in the chamber prior measurement start (settling time) for 5 min.

Leica TCS SP5II confocal laser scanning microscope (*Leica Microsystems CMS*
with a 63× lens (*HCX PLAPO Lambda blue 63*). Two

leaves were collected on 11 DAT (cv. Suntella) and 12 DAT

was performed using fresh hand-made cross sections of a

660 to 705 nm, at a room temperature. The pinhole was

z

as grana optical cross sections. The height of grana

z

between the samples, using *Leica SP5II* software. Image

3D-reconstruction of grana was performed using *ImageJ Fiji 3D* viewer software (Schindelin *et al.* 2012). *Handy*

PEA *Hansatech Instruments Ltd.* UK). Measurements were made *in vivo* on leaves of

stress conditions and leaves from the second pair, which

$^{-2}$ s^{-1}

1.0). Measurements were conducted in the middle part of

were derived from 15–37 measurements per treatment at each term per each cultivar.

Data from PF measurements were used in JIP-test *see* Cetner *et al.* *cf.* Strasser *et al.*

$_O$ = $F_{0.05ms}$

and F_m $_{Fm}$

$_0$

$_A$ reduction events between time zero (0) and T_{Fm}

$_{P0}$

$_{E0}$

$_{R0}$

$_A^-$ –

$_{E0}$

$_B$ $_{R0}$ $_A$

$_0$

$_A^-$ per RC – ET_0

$_0$

$_B$ – PI_{abs} – and until the reduction of PSI acceptors – PI_{tot}

$_0$.

Statistics: Formulas used for calculations of the JIP-test parameters have been presented elsewhere (Cetner *et al.* *cf.* Strasser *et al.* 2004). The number of repetitions is indicated for each of the performed measurements, and the means and calculated standard error of mean (SEM) are *R software* (*RStudio* *Microsoft Excel* (*Microsoft*, USA).

Pairwise Multiple Comparison Procedures (*Holm-Sidak* method).

Results

Foliar chemical composition: Total phosphorus concen-

2006). In the foliage of both the cultivars used in this

decrease in total P amount was observed, with the lowest $^{-1}$ $^{-1}$ (Suntella) on 12 DAT (Table 3S, *supplement*). Although P concentration was lower in the stressed plants as compared to the control plants, it remained within the above mentioned optimal range during the stress conditions. After the

of stressed plants of both the cultivars was higher as compared to control plants. Moreover, in the case of cv. Suntella, P concentration reached the highest value on 19 DAT plants (Fig. 2*A*). Intercellular CO_2 concentration (C_i) signi-

27 DAT (Fig. 2*A*).

In the case of cv. Suntella, P_N of the control plants
$_2$) m^{-2} s^{-1}
$_2$) m^{-2} s^{-1} on the 33rd d of vegetation (17

of vegetative period (data not shown). P-def plants of cv. Suntella had the P_N at the level of the control plants

DAT (Fig. 2

[redacted]

Fig. 3. Comparative data concerning 2D- and 3D-images of grana structures as well as Chl *a* *z*
A–C *D–F*). *Left column*: Confocal 2D-images
B,*C*,*E*,*F*) grana structures are less distinguishable as compared to the control sample (*A*,*D*
C,*F*
Middle column
(*B*,*C*,*E*,*F* *C*,*F*
Right column *z*
(*C*,*F*)] are shorter in size than those of the control sample.

within the chloroplasts of the control plants (Fig 3*A*,*D*).

of cv. Fluo (Fig 3*B*,*C*) and after 11 DAT in the case of cv. Suntella (Fig. 3*E*,*F*) resulted in the appearance of

spaces coincided with reduction of grana number per

Fig. 3). Three-dimensional reconstructions of grana revealed their uniform distribution within median optical

resulted in a lower number of grana structures as well as

of Chl *a* *z* *right column*

(*ca.*

Prompt fluorescence induction curves: Double normalization of Chl *a*

F_O and F_m allowed comparing the shapes of the curves recorded for P-def and control plants (Fig. 4). In both cultivars, a distinctive shape alteration was observed:

after the control solution with optimal nutrient content

(Figs. 4, 5).

The fading of the I-step was observed regardless of leaf age. However, in the case of cultivar Suntella, there were additional curve alterations observed that were

case of old leaves, a slight increase in Chl *a*

the curve from F_O to F_J

the J-step, as compared to that in the control sample.

JIP-test: Recorded Chl *a*

see e.g., Cetner *et al.*

much more pronounced in cv. Suntella. In both cultivars,

nutrient thus, it is relocated from the older leaves to the area of new growth. Therefore, the old leaves as compared

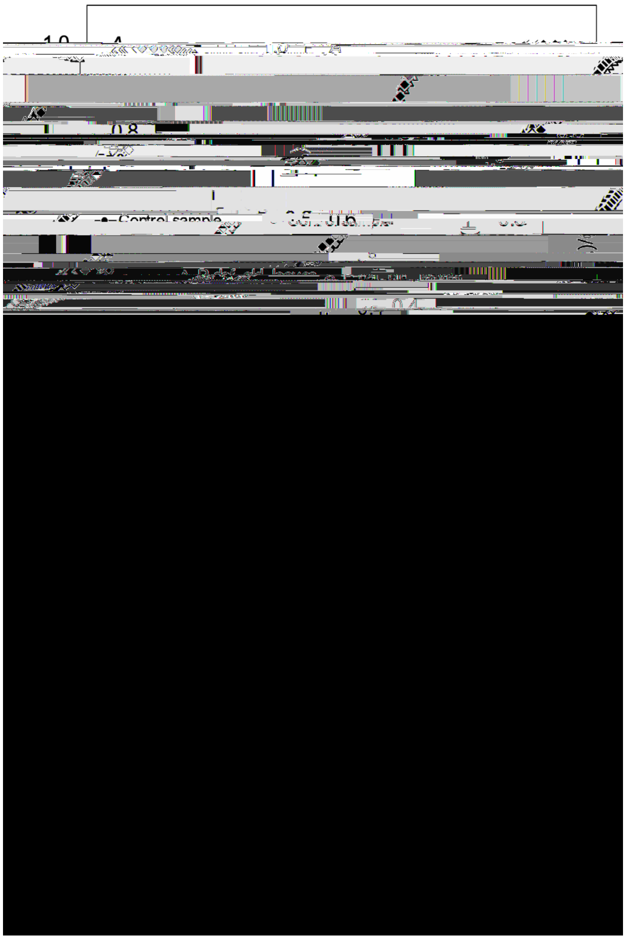

a

plants (on 13th

Raphanus sativus var. *sativus* *A* *B*) presented

$_t$ – F_O

(F_m – F_O). Mean values were derived from 15–37 measurements.

The increase in values of several parameters was observed in the old leaves. This included the followings: F_O, which indicates detachment of PSII Chl antenna *et al.* $_0$, net rate $_A$ reduction events (Strasser *et al.*

$_0$

$_A^-$ (ET_0

until PSI acceptors (RE_0

$_{P0}$

$_{E0}$

$_{R0}$

$_A$ $_{E0}$) were reduced.

$_A$ reducing RCs per PSII Chl

$_B$ (PI_{abs}) and until the reduction of PSI acceptors (PI_{tot}) were reduced. The

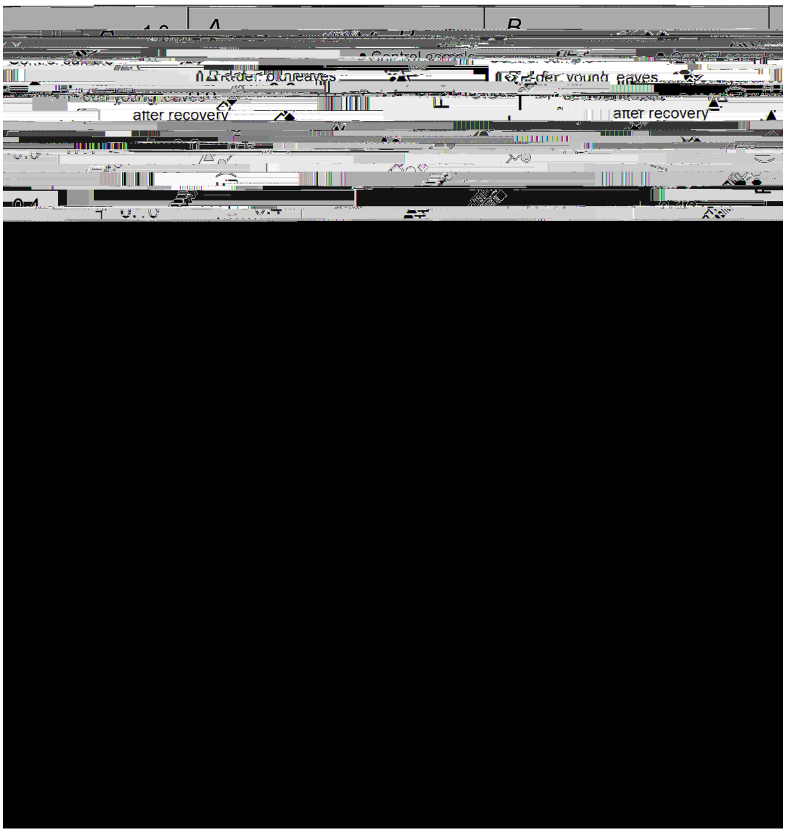

Fig. 5. Changes in the relative shape of chloro-
a

bottom leaves (*A,C*
(*B,D* th d

Raphanus
sativus var. *sativus* *A,B*)
C,D
$_t$ – F_j
($F_m – F_j$) (*left axis*

(*right axis*). Mean values were derived from 15–37 measurements.

B R0)
supplement).

Increases in both F_O and F_m parameters were observed

0) also

RC (TR_0 0 0
A

P0 E0 R0

A E0)

B R0).

Therefore, PI_{tot} was reduced, but no change was observed in PI_{abs}.

A reducing)

conservation decreased, which is in agreement with the *et al.* (2004).

Discussion

et al. (2015) on other plants.

Decreases in the P_N as well as in g_s (Fig. 2) indicate

et al. 2008).
C_i suggests that a

CO_2 assimilation in P-def plants (Lin *et al.* 2009). Weng *et al.* (2008) suggested that the decline in P_N might be due

The observed changes in chloroplasts ultrastructure
i.e.,

under stress conditions, and changes in the shape of Chl
et al. 2010).

et al.
et al. 2010). In our research, we observed a

et al. (2015)
a

Raphanus sativus var. *sativus*

Pairwise Multiple Comparison Procedures (*Holm-Sidak* * ns.

Parameter	Old leaves		Young leaves	
	CS	–P	CS	–P
Fluo HF1				
$F_O = F_{0.05\ ms}$	606.900 ± 48.933	959.125 ± 47.379*	728.815 ± 51.580	953.129 ± 48.137*
F_m	3,100.333 ± 64.146	3,111.094 ± 62.109ns	2,963.185 ± 67.616	3,475.323 ± 63.103*
T_{Fm}	268.000 ± 13.517	259.375 ± 13.088ns	301.852 ± 14.248	281.290 ± 13.297ns
M_0	0.708 ± 0.039	0.941 ± 0.038*	0.846 ± 0.041	0.844 ± 0.039ns
N	19.290 ± 0.796	21.821 ± 0.771ns	21.159 ± 0.839	20.933 ± 0.783ns
$_{P0}$	0.804 ± 0.018	0.687 ± 0.017*	0.736 ± 0.019	0.728 ± 0.017ns
$_{E0}$	0.473 ± 0.017	0.377 ± 0.016*	0.386 ± 0.018	0.419 ± 0.016ns
$_{R0}$	0.209 ± 0.007	0.164 ± 0.007*	0.199 ± 0.008	0.194 ± 0.007ns
$_{E0}$	0.586 ± 0.014	0.538 ± 0.014*	0.516 ± 0.015	0.570 ± 0.014*
$_{R0}$	0.447 ± 0.016	0.448 ± 0.016ns	0.521 ± 0.017	0.473 ± 0.016*
	0.478 ± 0.014	0.349 ± 0.014*	0.429 ± 0.015	0.382 ± 0.014*
TR_0	1.702 ± 0.036	2.016 ± 0.034*	1.733 ± 0.037	1.940 ± 0.035*
ET_o	0.994 ± 0.023	1.075 ± 0.022*	0.888 ± 0.024	1.096 ± 0.022*
RE_0	0.443 ± 0.016	0.478 ± 0.016ns	0.457 ± 0.017	0.517 ± 0.016*
PI_{abs}	3.040 ± 0.188	1.374 ± 0.182*	1.848 ± 0.198	1.713 ± 0.185ns
PI_{tot}	2.395 ± 0.152	1.007 ± 0.147*	1.963 ± 0.161	1.459 ± 0.150*
$_0$	284.890 ± 6.481	308.949 ± 6.275*	302.340 ± 6.832	342.180 ± 6.376*
Suntella F1				
$F_O = F_{0.05\ ms}$	627.233 ± 37.848	1066.480 ± 41.460*	671.214 ± 39.176	768.577 ± 40.655ns
F_m	3,078.167 ± 53.894	2,699.120 ± 59.038*	3,210.893 ± 55.785	3,502.385 ± 57.891*
T_{Fm}	293.000 ± 11.552	330.400 ± 12.654ns	313.929 ± 11.957	313.077 ± 12.409ns
M_0	0.684 ± 0.035	0.978 ± 0.038*	0.710 ± 0.036	0.643 ± 0.038ns
N	20.244 ± 0.839	26.694 ± 0.919*	21.925 ± 0.868	20.316 ± 0.901ns
$_{P0}$	0.796 ± 0.017	0.587 ± 0.018*	0.790 ± 0.017	0.779 ± 0.018ns
$_{E0}$	0.456 ± 0.015	0.322 ± 0.017*	0.442 ± 0.016	0.494 ± 0.016*
$_{R0}$	0.205 ± 0.006	0.147 ± 0.007*	0.232 ± 0.006	0.212 ± 0.007*
$_{E0}$	0.571 ± 0.012	0.523 ± 0.013*	0.556 ± 0.012	0.633 ± 0.013*
$_{R0}$	0.454 ± 0.014	0.488 ± 0.015ns	0.536 ± 0.014	0.429 ± 0.015*
	0.510 ± 0.014	0.307 ± 0.015*	0.505 ± 0.014	0.447 ± 0.015*
TR_0	1.583 ± 0.034	2.011 ± 0.037*	1.585 ± 0.035	1.751 ± 0.036*
ET_0	0.899 ± 0.017	1.033 ± 0.018*	0.875 ± 0.017	1.107 ± 0.018*
RE_0	0.404 ± 0.010	0.498 ± 0.011*	0.463 ± 0.010	0.475 ± 0.010ns
PI_{abs}	2.941 ± 0.183	1.006 ± 0.200*	2.718 ± 0.189	2.861 ± 0.196ns
PI_{tot}	2.401 ± 0.154	0.771 ± 0.169*	3.004 ± 0.160	2.177 ± 0.166*
$_0$	312.516 ± 6.170	286.533 ± 6.759*	332.868 ± 6.387	341.205 ± 6.628ns

induction curves as distinguishable in P-def plants and can be used as bioindicator to predict and monitor plant nutrient status. The sigmoidal rise from the step I to P has

cf.

et al.

et al. (2005) observed the disappearance of

cf.

b_6f 2

b_6f

to PSI (Rich *et al.* *et al.* 2005). On the

from the Fe-

et al. *et al.* 2005). Considering the above case of P-def plants can be connected to the disturbances

cf. *et al.* *et al.* 2015). Furthermore, several studies (*see e.g.*, Hamdani *et al.* 2015) have shown a clear relationship of the slope of

as well as recovered plants.

a

detachment (increased F_O) and the decrease in active

A

P0 E0) and

R0) along with the

A E0), as the main causes of ETC

i.e., LHCII uncoupling and inactivation of RCs, are connected with mechanisms protecting PSII against photoinhibition *et al.* 2008, Belgio *et al.* 2012, Kalaji *et al.*

indicators.

(Strasser *et al.* 2004). The inactivation of OEC could be connected with the appearance of a positive K-band at *et al.* 2010, Stirbet *et al.* 2014, Kalaji *et al.* 2016). Since there was no clear K-band observed in the induction curves revealed for P-def plants (data not

at PSII acceptor side generates the transmembrane pH

2 and

b_6f

et al.

leads to a rapid decrease in stromal Pi, to the point where

Jacob J., Lawlor D.W.: *In vivo*

6: 785-795, 1993.

46: 5534-5541, 2007.

Arabidopsis thaliana
cence. – J. Photoch. Photobio. B **98**: 180-187, 2010.

84: 631-657, 2015.

et al. *a*

38: 102, 2016.

et al

132: 13-66, 2017.

et al

in vivo

122: 121-158, 2014.

Lin Z.H., Chen L.S., Chen R.B. *et al.*: CO_2 assimilation, ribulose-

Biol. **9**: 43, 2009.

a

132: 650, 2005.

Agronomic phosphorus imbalances across the world's croplands. – P. Natl. Acad. Sci. USA **108**: 3086-3091, 2011.

et al. (ed.): Plant Nutrients and Abiotic Stress Tolerance. Pp. 171-190. Springer, Singapore 2018.

et al.: Light absorption

organisms. – Chem. Rev. **117**: 249-293, 2017.

a in vivo

Chlorella pyrenoidosa

Chlorella pyrenoidosa **9**: 1-35, 1969.

and II. – Annu. Rev. Plant Biol. **57**: 521-565, 2006.

bf **1058**: 312-328, 1991.

Sorghum

a

Sci. **100**: 615-618, 2004.

In: Schoefs B. (ed.): Plant Cell Compartments – Selected Topics. Pp. 41-104. Research Signpost, Kerala 2008.

nd

2006.

a

BBA-Bioenergetics **1706**: 250-261, 2005.

Schindelin J., Arganda-Carreras I., Frise E. *et al.*: Fiji: an open-

9: 676-682, 2012.

et al.:

to changes in leaf manganese status. – Front. Plant Sci. **7**: 1772, 2016.

2019.

BBA-Bioenergetics **1817**: 1134-1151, 2012.

a

A personal perspective of the thermal phase, the J-I-P rise. – **113**: 15-61, 2012.

a

79: 291-323, 2014.

a